Three dimensional fully polarimetric W-band ISAR imagery of scale-model tactical targets using a 1.56THz compact range.

Thomas M. Goyette[*a], Jason C. Dickinson[a], Jerry Waldman[a], William E. Nixon[b]

[a]Submillimeter-Wave Technology Laboratory, University of Massachusetts Lowell, 175 Cabot St., Lowell, MA 01854

[b]U.S. Army National Ground Intelligence Center, 2055 Boulders Road, Charlottesville, VA 22911

ABSTRACT

Using the high-frequency terahertz compact range developed recently for measurement of polarimetric return of scale models of tactical targets, we have developed several techniques to produce three-dimensional data sets. Fully polarimetric three-dimensional ISAR data has been collected on several 1/16th scale model tactical targets in free space at individual look angles. The three-dimensional scattering coordinates are calculated by viewing the target through a two-dimensional angular aperture in both azimuth and elevation while simultaneously performing a linear frequency chirp to measure the down-range coordinate. Due to the high frequency of W-band radar, this technique produces high-resolution cross-range images from relatively small (approximately 1 degree) angular integrations. Several techniques for calculation of the three-dimensional coordinates have been developed. In addition to the technique described above, a new method utilizing the phase change of the scattering centers due to differentially small changes in angle will be described. Data collected using this technique can be processed to produce three-dimensional scattering information similar to that obtained by monopulse systems. Results from this analysis will be shown.

Keywords: Sub-millimeter, Radar, Imagery, Modeling.

1. INTRODUCTION

Due to the continuing evolution of radar systems that require detailed target signature information, the need for high quality radar cross-section (RCS) data has been growing steadily. This data is commonly used in algorithms for target recognition, acquisition, tracking and for validation of computational radar scattering prediction codes. The data of interest to these programs include synthetic aperture radar (SAR) and high-range-resolution (HRR) target profiles. The U. S. Army National Ground Intelligence Center (NGIC) Expert Radar Signature Solutions (ERADS) program including the Submillimeter-Wave Technology Laboratory (STL) at UMass Lowell have developed compact ranges to measure the radar return of scale models of targets of interest. Target signature data is collected by measuring the scaled models (typically 1/16th or 1/35th scale) at proportionally scaled frequencies. The ERADS compact ranges currently model frequencies from UHF up to W-Band.

Sinclair thoroughly addressed the mathematics and theory of using scale models and proportionally scaled wavelengths to study the scattering of electromagnetic radiation in 1948.[1] While this technique had been successfully used at lower frequencies, it was not until 1980 that the method was adapted for use in the sub-millimeter wavelength region.[2] In order to measure targets using these high frequencies a very high fidelity scale model is required which models not only the features of the target but also the dielectric properties. For this purpose, the Materials Research Lab at STL specializes in developing dielectric materials to match the properties of full-scale targets. Studies have shown that data taken on high quality 1/16th scale models compare well with the same data taken on the full-scale targets.[3]

Since monopulse radar systems, which provide angular information on targets, are becoming more common, there is a need for data sets that provide three-dimensional (3D) coordinates of the target's scattering centers. In the past,

[*] Correspondence: Email: Thomas_Goyette@uml.edu; Telephone: (978) 458-3807; Fax: (978) 452-3333.

Report Documentation Page

Form Approved
OMB No. 0704-0188

1. REPORT DATE	2. REPORT TYPE	3. DATES COVERED
SEP 2003		**00-00-2003 to 00-00-2003**

4. TITLE AND SUBTITLE	5a. CONTRACT NUMBER
Three dimensional fully polarimetric W-band ISAR imagery of scale-model tactical targets using a 1.56THz compact range	5b. GRANT NUMBER
	5c. PROGRAM ELEMENT NUMBER
6. AUTHOR(S)	5d. PROJECT NUMBER
	5e. TASK NUMBER
	5f. WORK UNIT NUMBER
7. PERFORMING ORGANIZATION NAME(S) AND ADDRESS(ES) **University of Massachusetts Lowell,Submillimeter-Wave Technology Laboratory,175 Cabot Street,Lowell,MA,01854**	8. PERFORMING ORGANIZATION REPORT NUMBER
9. SPONSORING/MONITORING AGENCY NAME(S) AND ADDRESS(ES)	10. SPONSOR/MONITOR'S ACRONYM(S)
	11. SPONSOR/MONITOR'S REPORT NUMBER(S)

12. DISTRIBUTION/AVAILABILITY STATEMENT
Approved for public release; distribution unlimited

13. SUPPLEMENTARY NOTES

14. ABSTRACT

15. SUBJECT TERMS

16. SECURITY CLASSIFICATION OF:			17. LIMITATION OF ABSTRACT	18. NUMBER OF PAGES	19a. NAME OF RESPONSIBLE PERSON
a. REPORT **unclassified**	b. ABSTRACT **unclassified**	c. THIS PAGE **unclassified**		**9**	

compact ranges used spot scanning of the target with a swept-frequency radar beam focused to sub-resolve the target and provide 3D scatterer data.[4] In this paper we will present the results of measurements that provide fully polarimetric 3D data by illuminating the entire target and generating a two-dimensional solid angle synthetic aperture. Additionally, we have employed an interferometric technique in which the phase change due to a very small change in angle of the target is used to calculate the three-dimensional coordinates, without the need to view the target through a complete solid angle. We will show that data collected using this technique can be processed to provide equivalent information obtained by radar systems employing monopulse techniques.

2. THE 1.56THZ COMPACT RADAR RANGE

The 1.56THz W-band compact range has been described previously[5], therefore only a brief description will be presented here. Figure 1 shows an outline of the compact range. The sources for the transmitter and receiver consist of two optically pumped lasers producing sub-millimeter radiation at approximately 191.8 m, giving a laser frequency of 1.56THz. These ultra-stable lasers drive corner cube mounted Schottky diodes to mix with the output of a tunable 10-20GHz microwave sweeper. The 1/16th scale model is illuminated by the resulting sideband, which is radiated out from the corner cube diodes. Table 1 shows a list of the radar parameters for the 1.56Thz compact range along with the full-scale equivalent parameters. Only the full-scale parameters will be used in the following discussion.

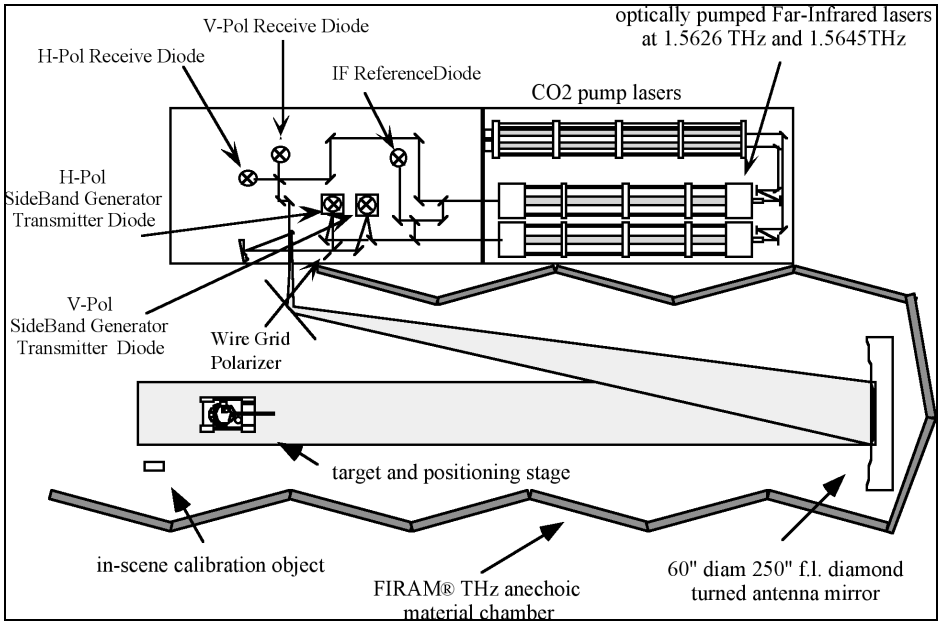

Figure 1. Diagram of the 1.56THz compact radar range.

1.56THz Compact Range	**(Full Scale)**
1546 GHz Start Frequency	(96.6 GHz Full scale)
8 GHz Bandwidth	(500 MHz Full Scale)
0.74” Range Resolution	(11.6” Full Scale)
20” Two Way Beam Width (-3dB)	(26.6’ Full Scale)
Far Field Beam, 0.3˚ bistatic	
Fully Polarimetric HH, HV, VH, VV amplitude and phase	

Table 1. Radar parameters for the 1.56THz compact range when modeling W-Band.

3. THREE DIMENSIONAL ISAR IMAGING

Mensa has given a detailed description of Inverse Synthetic Aperture Radar (ISAR) imaging,[6] the relevant features of which are briefly summarized. Consider the effect of rotation on a target as shown in Figure 2. A scatterer at distance *d* from the transceiver will have a round trip phase *(□)* which will be a function of the frequency*(f)* and distance *(d)*, □=4□df/c. If the object is also rotated about a central point the change in phase will vary as a function of its crossrange location. Therefore, a linear change in frequency will produce a linear change in phase of the scatterer as will a smooth rotation. This type of data can then be processed with standard Doppler techniques. By using a Fourier transform the Doppler frequencies contained in the data can be separated from one another. The Fourier transform of the frequency information will yield down range coordinates while the Fourier transform of rotation data will give crossrange information. To produce three-dimensional data the target is measured through a two-dimensional aperture while at the same time performing a linear sweep in frequency. To build the two-dimensional aperture the target is measured at a series of evenly spaced azimuth and elevation angles. Three separate Fourier transforms are then performed to calculate the *x, y,* and *z* coordinates of the scattering centers.

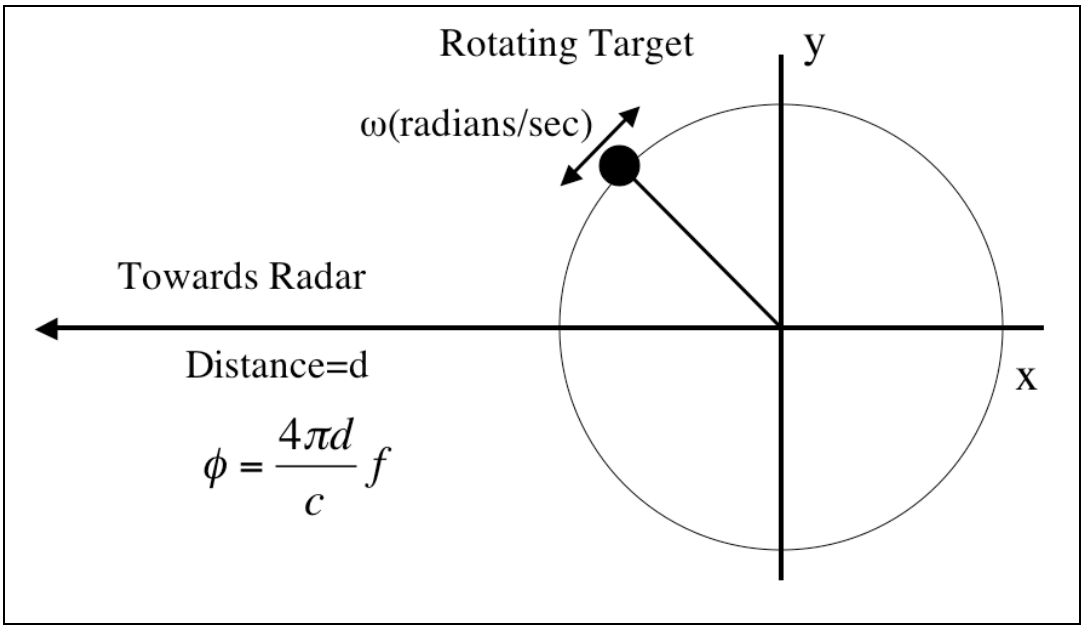

Figure 2. The phase change of a target as a function of position and radar frequency.

Figure 3 shows the four targets, which have been studied using 3D imaging. The tanks studied are the T55, M48, T72 and Leopard. The tanks were mounted in the compact range and HRR data was collected over a 1.28˚x1.28˚ solid angle using a 0.01˚ angular increment. This method produced 3D images with voxel element sizes of 2.8”x2.8”x11.6”. Using 0.5-second duration linear frequency chirps then requires approximately 2 hours of data collection to produce one view angle of 3D data. This integration time also gives an approximately –50dBsm/voxel noise floor for the 3D data set.

Imagery from the 3D data sets for the various targets are shown in Figures 4-8. Each of these figures shows the fully polarimetric front view (azimuth/elevation) of the targets in HH, HV, VH, and VV polarization channels. Additionally, the slant plane (ISAR) view and side view are also displayed. For ease of viewing, only the HH polarization channel is displayed for slant plane and side view since the other polarization states are very similar and the addition of the extra channels makes the display much more difficult to read. It is seen that the integration across a 1.28˚x1.28˚ solid angle results in very good crossrange resolution in the front view of Figures 4-8. It is useful to note that in Figures 5 - 8 the individual wheels can also be clearly seen. The amount of scattering seen from the Leopard in Figure 6 is also interesting since the other tanks all show major scattering coming from the turret, while scattering from the Leopard’s turret is relatively low with most of the radar return coming from the front body of the tank. By looking at

the slant plane view alone it is not possible to see these differences. The T55 data set in Figure 8 shows the most scattering in general from the entire tank surface. This imagery demonstrates the ability to gain better understanding of complex scattering phenomena

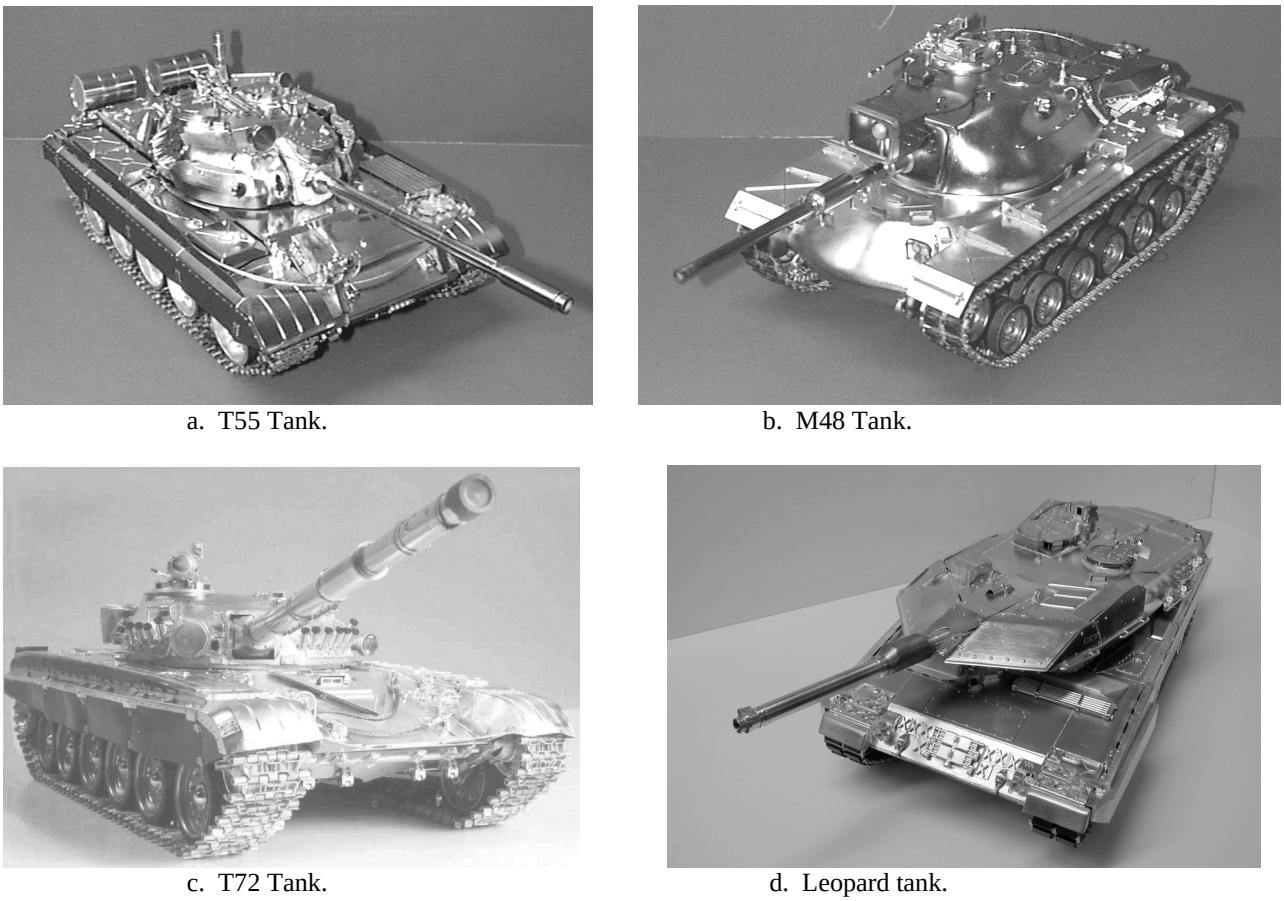

a. T55 Tank. b. M48 Tank.

c. T72 Tank. d. Leopard tank.

Figure 3. Photographs of scale modeled tanks used in this study.

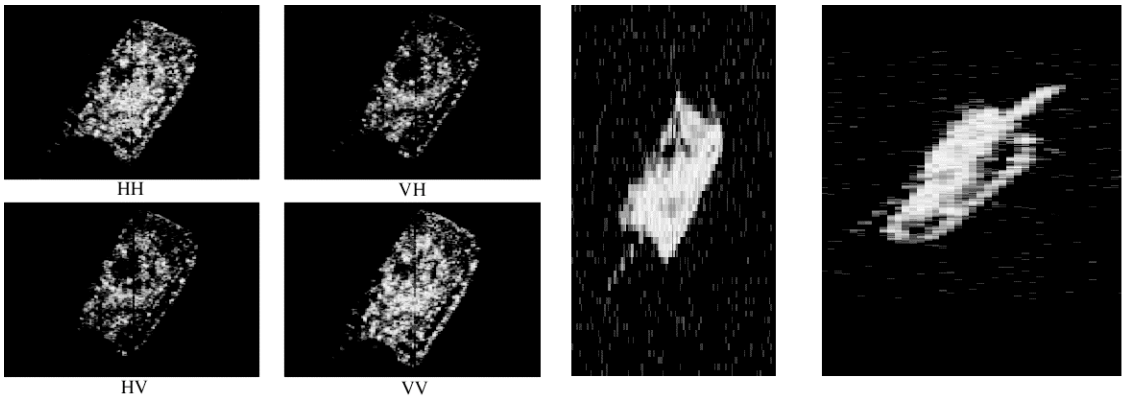

a b c

Figure 4. Three-dimensional data on the T72 tank model viewed at 40˚ elevation and 30˚ azimuth with turret turned 9˚ clockwise; (a) Front View, (b) HH Slant Plane View, (c) HH Side View. Minimum pixel value is –45dBsm.

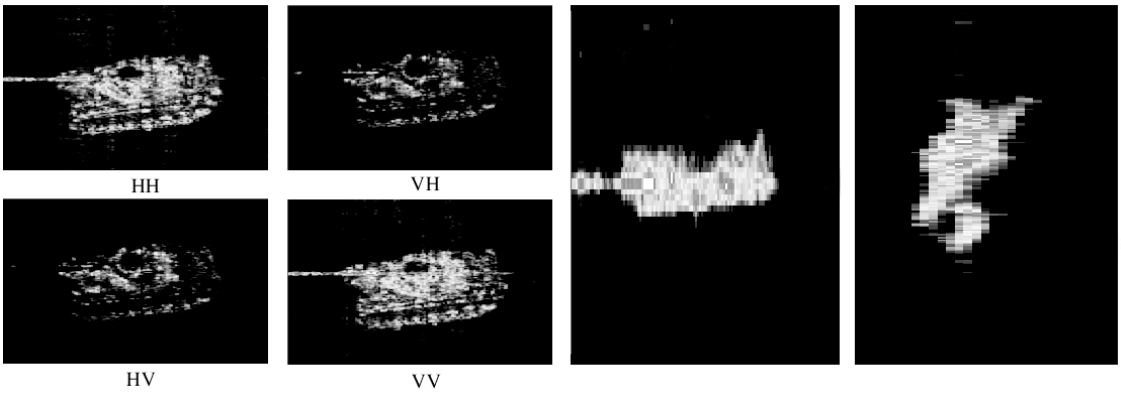

a b c

Figure 5. Three-dimensional data on the T72 tank model viewed at 40˚ elevation and 80˚ azimuth with turret turned 9˚ clockwise; (a) Front View, (b) HH Slant Plane, (c) HH Side View. Minimum pixel value is –45dBsm.

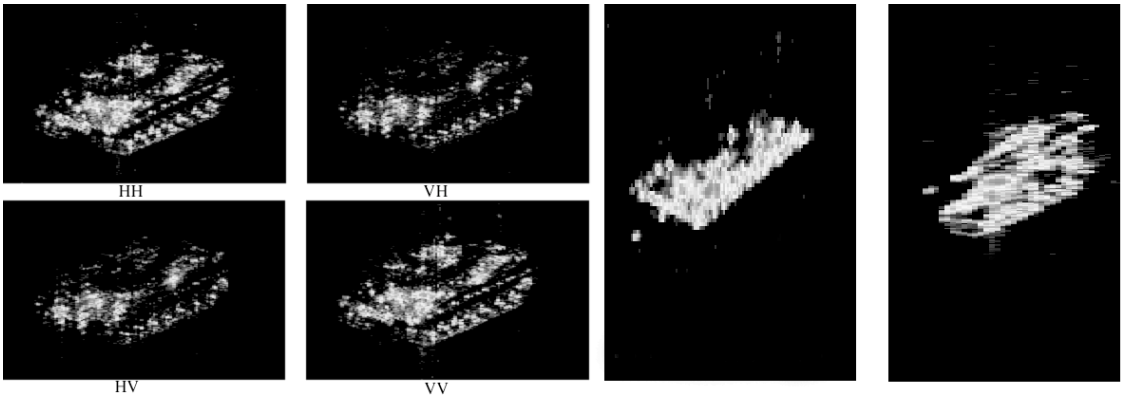

a b c

Figure 6. Three-dimensional data on the Leopard tank model viewed at 15˚ elevation and 40˚ azimuth; (a) Front View, (b) HH Slant Plane View, (c) HH Side View. Minimum pixel value is –45dBsm.

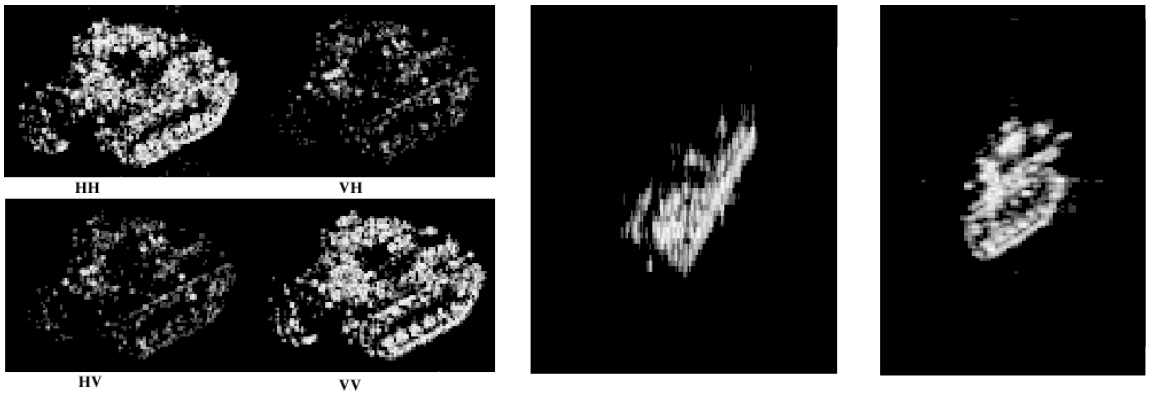

a b c

Figure 7. Three-dimensional data on the M48 tank model viewed at 15˚ elevation and 30˚ azimuth; (a) Front View, (b) HH Slant Plane View, (c) HH Side View. Minimum pixel value is –50dBsm.

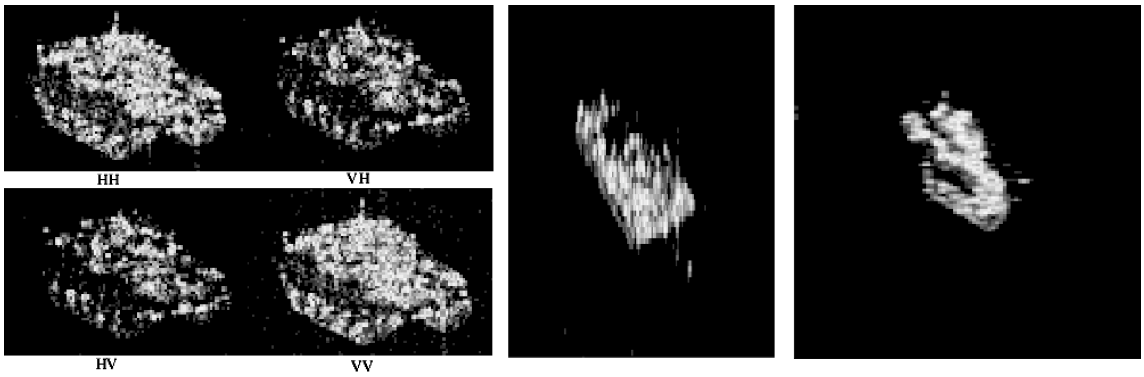

a b c

Figure 8. Three-dimensional data on the T55 tank model viewed at 15˚ elevation and 330˚ azimuth; (a) Front View, (b) HH Slant Plane View, (c) HH Side View. Minimum pixel value is –50dBsm.

4. MONOPULSE 3D IMAGING

In addition to the three dimensional ISAR techniques described in Section 3, previous works have suggested other methods to estimate the positions of scatterers on a target.[7] One such method mentioned in Ref(7), known as monopulse imaging, involves using monopulse radar, which can measure the angular deviation of an object from the center of the radar system. A detailed description of monopulse systems can be found in Ref(8) therefore, we will be brief here.

Figure 9 shows a simplified diagram of a phase monopulse system. In this diagram antennas A and B are separated from one another by a distance L and have parallel and overlapping fields of view. A target located at a range R from the center of the antennas will have a difference in phase between the two channels whose sign is dependent on the scatterer being located above or below the null axis (point of zero phase difference). It can easily be shown that if the range to the target is much greater than the separation between the antennas, the phase difference registered between antenna A and B is given to a good approximation by Equation 1. Therefore, the change in phase of the target varies proportionally with the target's crossrange position r_y.

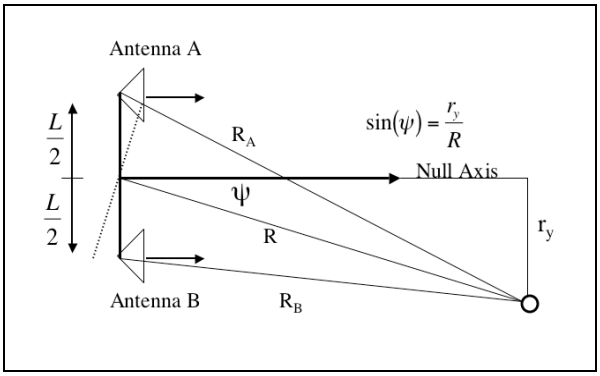

Figure 9. Geometry of monopulse radar system.

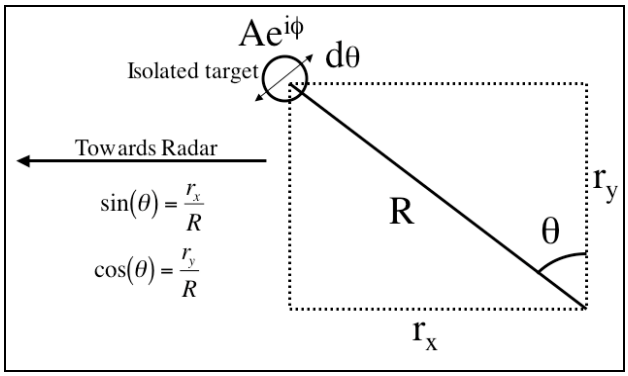

Figure 10. Geometry of Differential Phase radar.

$$\Delta\phi = 2\pi\frac{L}{\lambda}\sin(\theta) = 2\pi\frac{L}{\lambda}\frac{r_y}{R} \tag{1}$$

This technique can be adapted for use in a compact radar range by again utilizing the phase information of the target. Figure 10 shows the basic geometry for an isolated scatterer. This isolated target has a phase in the direction of

the radar given by Equation 2 with respect to an arbitrary point of rotation. It is useful to note that Equations 1 and 2 represent single pass phases of the radars beam. For double passes the equations must be multiplied by a factor of two. In this discussion we will limit ourselves to describing the single pass results. However, the equations can be modified by the relevant multiplicative factors to account for any combination of transmitter/receiver system. Taking a derivative, Equation 3 shows that the variation of phase for an individual scatterer is directly proportional to the crossrange distance out from the point of rotation.

$$\Delta\phi = 2\pi \frac{R\sin(\Delta\theta)}{\lambda} \tag{2}$$

$$\frac{\partial\phi}{\partial\theta} = 2\pi \frac{R\cos(\Delta\theta)}{\lambda} = \frac{2\pi}{\lambda} r_y \tag{3}$$

Therefore, if a careful measurement is made of the phase change of the target under differential changes in angle θ, the crossrange position can be calculated in a similar way to that of phase monopulse. If we were to require that the phase change between the two methods be identical, a constraint on $\Delta\theta$ can be calculated from Equations 1 and 3 such that

$$\Delta\theta = \frac{L}{R} \tag{4}$$

Since R>>L this can be interpreted as constraining $\Delta\theta$ to match the angular perspective of the two antennae in Figure 9 at range R. The same result also holds when both radar systems (Figures 9 and 10) involve a double pass phase change. It has been noted in Ref(7) that if there are multiple unresolved scatterers involved in this calculation, there may be a false representation of the calculated coordinate. Since the technique will be applied to ISAR images this will mitigate the ambiguity, and the results will improve with higher resolution data sets.

As an example, this method has been used on one of the data sets from Section 3. Since the three-dimensional data has already been taken, the phase comparison can be done simply by comparing the phase of two ISAR images contained in this data set separated by a small elevation angle. The T55 data set, with a large number of scattering sites, offers an ideal opportunity to calculate the elevation coordinate by using the differential phase (Equations 2 and 3) technique, which has been shown above to be equivalent to monopulse imaging. The 3-D image that is formed can then be compared to the results of the 3-D ISAR.

Figure 11 shows two ISAR images for the T55 tank taken at identical aspect angles but at different elevation angles (15.000˚ elevation and 15.020˚ elevation respectively). By using the two data sets of Figure 11 it is possible to perform a point by point difference in phase between each pixel in Figure 11(a) and Figure 11(b). Using Equation 3 the elevation crossrange of the scattering centers can be calculated. Since the downrange resolution of the system is 11.9", the change in elevation angles over such a small increment will not permit the scattering centers to shift from one range cell to another, thereby satisfying the condition imposed by Equation 3 that the change in angle be a differential one.

a b

Figure 11. ISAR images of the T55 tank at 330˚ azimuth; a) 15.000˚ elevation, b) 15.020˚ elevation.

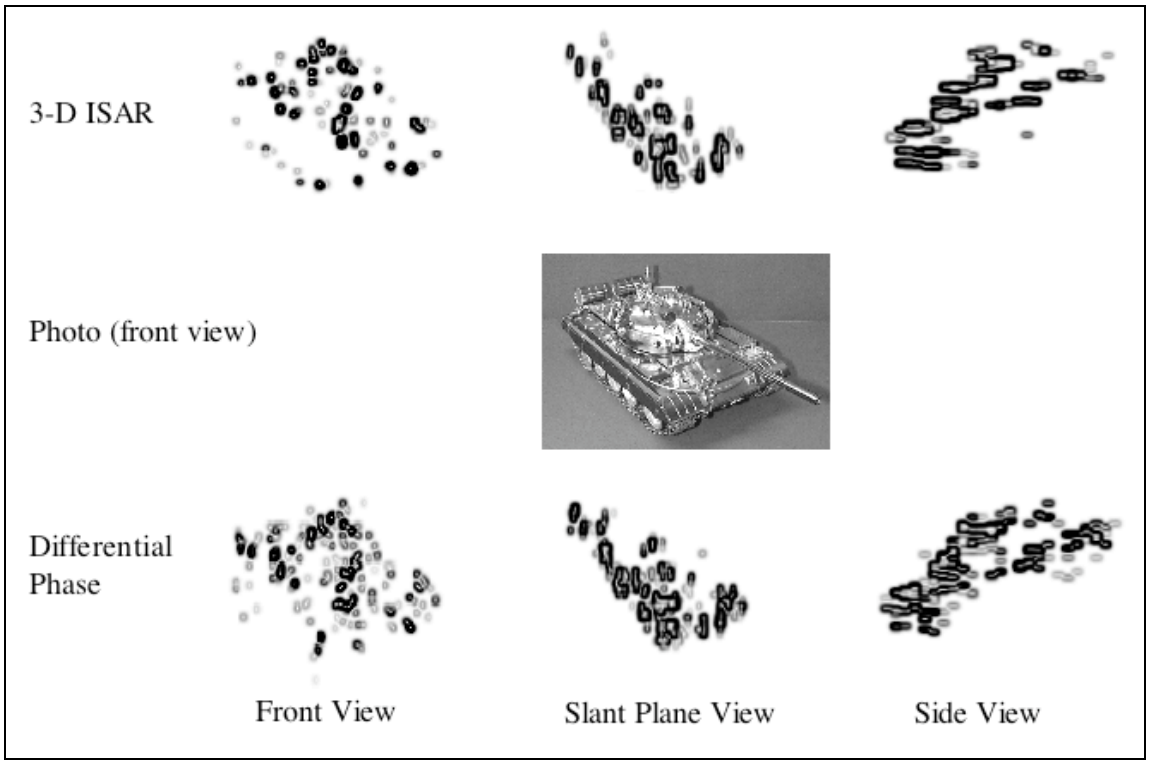

Figure 12. Contour plot of 3D data calculated by 3D ISAR (upper figure) and by the differential phase method (lower figure) in front view, slant plane view and side view. Scatterers are plotted down to the –20dBsm level.

The calculated three-dimensional scattering centers are shown in Figure 12 for both the 3D ISAR method and the differential phase method. Also shown in this figure is a photograph of the T55 model tank at approximately the view angle. While the individual ISAR data sets have a noise floor of –30dBsm, the data in Figure 12 is displayed down to a level of –20dBsm. This level is due to the requirement of the monopulse calculation that the phase be relatively stable. It is found that limiting signals to levels approximately 10dB above the noise floor is sufficient to satisfy that condition. An examination of Figure 12 shows that the estimation of the positions of scattering centers derived by the differential phase technique match reasonably well with the 3D ISAR data set. The major scatterers in the front, top and side views appear to be well reproduced. There are some differences, typically at the lower levels. However, these differences are most likely due to unresolved scattering in the elevation direction. It is encouraging to note that this simple two-point interferometric method does seem to reproduce the 3D ISAR images, with only small fraction of the data.

5. SUMMARY

Fully-polarimetric 3D radar scattering data has been collected on four $1/16^{th}$ scale model tanks. High-resolution W-Band 3D ISAR images were formed by collecting HRR profiles of the targets through a 1.28°x1.28° solid angle in azimuth and elevation stepped by 0.01°. A technique has also been presented that calculates the 3D coordinates by comparing the phase change of scatterers in ISAR images at slightly different elevation angles. It has been shown that data collected using this technique can be processed to be equivalent to monopulse methods that measure the phase difference between two antennae to achieve the same result. Since these measurements have been successful at W-band, it should be possible to apply the same technique at lower radar frequencies under similar conditions.

REFERENCES

1. G. Sinclair, "Theory of models of electromagnetic systems", Proceedings of IRE, Vol **36**, No. 11, p1364-1370, Nov. 1948.
2. J. Waldman, H. R. Fetterman, W. D. Goodhue, T. G. Bryant, and D. H. Temme, "Sub-millimeter modeling of millimeter radar systems", Proc. SPIE, Vol **259**, p152, 1980.
3. R. H. Giles, W. T. Kersey, M. S. McFarlin, R. Finley, H. J. Neilson, and W. E. Nixon, "A Study of Target Variability and Exact Signature Reproduction Requirements for Ka-Band Radar Data", *Proceedings of SPIE, Signal Processing, Sensor Fusion and target Recognition X*, Vol **4380**, p117-126, 2001.
4. G.B. De Martinis, T.M. Goyette, M. Coulombe, J. Waldman, "A 1.56 THz Spot Scanning Radar Range for Fully Polarimetric W-Band Scale Model Measurements", Proceedings of the 22nd Annual Symposium of the Antenna Measurements and Techniques Association, October 2000, Philadelphia PA.
5. T. M. Goyette, J. C. Dickinson, J. Waldman, W. E. Nixon, and S. Carter, "Fully polarimetric W-band ISAR imagery of scale-model tactical targets using a 1.56-THz compact range", *Proceedings of SPIE, Algorithms for Synthetic Aperture Radar Imagery VIII*, Vol. **4382**, p229-240, 2001.
6. D. L. Mensa, *High Resolution Radar Imaging*, Artech House, Dedham, MA, 1981.
7. J. L. Kurtz and J. A. Scheer, *Radar Reflectivity Measurements: Techniques and Applications*, N. C. Currie Editor, Artech House, Norwood, MA, 1989.
8. D. K. Barton and S. A. Leonov, *Radar Technology Encyclopedia*, Artech House, Norwood, MA, 1997.